



Published in final edited form as:

*Curr Biol.* 2006 August 8; 16(15): 1559–1564.

## Tumor Formation via Loss of a Molecular Motor Protein

Manjari Mazumdar<sup>1,\*</sup>, Ji-Hyeon Lee<sup>1</sup>, Kundan Sengupta<sup>1</sup>, Thomas Ried<sup>1</sup>, Sushil Rane<sup>1</sup>, and Tom Misteli<sup>1,\*</sup>

<sup>1</sup>National Cancer Institute, National Institutes of Health Bethesda, Maryland 20892

### Summary

Aneuploidy has long been suggested to be causal in tumor formation. Direct testing of this hypothesis has been difficult because of the absence of methods to specifically induce aneuploidy. The chromosome associated kinesin motor KIF4 plays multiple roles in mitosis, and its loss leads to multiple mitotic defects including aneuploidy [1-5]. Here, we have taken advantage of the direct formation of aneuploidy in the absence of KIF4 to determine whether loss of a molecular motor and generation of aneuploidy during mitosis can trigger tumorigenesis. We find that embryonic stem cells genetically depleted of KIF4 support anchorage-independent growth and form tumors in nude mice. In cells lacking KIF4, mitotic spindle checkpoints and DNA-damage response pathways are activated. Down regulation or loss of KIF4 is physiologically relevant because reduced KIF4 levels are present in 35% of human cancers from several tissues. Our results support the notion that loss of a molecular motor leads to tumor formation and that aneuploidy can act as a primary trigger of tumorigenesis.

### Results

We sought to analyze the tumor potential of cells lacking the motor protein KIF4. To this end, we used a homogenous population of murine KIF4 KO embryonic stem (ES) cells generated by gene disruption via insertion of  $\beta$  near the 5' end of the gene (see the Supplemental Experimental Procedures available with this article online for details). KIF4 is located on the X chromosome, and male ES cells with a disrupted KIF4 gene are thus KIF4 null. Absence of KIF4 was confirmed by Western blot analysis and immunofluorescence microscopy (Figures S1A and S1B). Loss of KIF4 in murine ES cells leads to the expected multiple mitotic defects including chromosome misalignments, spindle defects, and aberrant cytokinesis (Figure 1A). In addition, a substantial population of KIF4 KO mitotic cells formed anaphase bridges (Figure 1B). Disruption of the KIF4 gene produces pronounced cytokinesis defects, and as a consequence, a large number of KIF4 KO cells were binucleate or had multiple nuclei including micronuclei. These defects were primary in nature and were not due to prolonged culturing of the cell lines in the absence of KIF4, because RNAi depletion in the parental mouse ES cells for as little as 16 hr yielded identical phenotypes (Figure 1A; [3]). SKY analysis of KIF4 KO cells revealed frequent numerical chromosome changes (Figure 1D). More than 70% of KIF4 KO cells were aneuploid, and chromosome numbers varied widely, from as low as 29 chromosomes to near diploid numbers. In comparison, parental control cells were invariably diploid. Although no recurrent chromosomal translocations were observed, nonclonal rearrangements occurred in 12 out of 30 KIF4 KO karyotypes (Figure 1D).

### KIF4 KO Cells Support Anchorage-Independent Growth and Tumor Formation

Having established the fact that KIF4 KO cells were aneuploid, we sought to determine whether they had tumor potential. When we tested KIF4 KO cells in a standard soft-agar anchorage-independent growth assay, they were able to form colonies as efficiently as the positive control

\*Correspondence: mazumdam@mail.nih.gov(M.M.);mistelit@mail.nih.gov(T.M.)

NIH-3T3 cells transformed by HA-Ras ( $400 \pm 38$  colonies/ $10^4$  cells versus  $350 \pm 90$  colonies/ $10^4$  cells) (Figure 2A). In the negative control, parental ES cells formed only  $131 \pm 55$  colonies/ $10^4$  cells, and nontransformed NIH-3T3 cells formed  $14 \pm 2$  colonies/ $10^4$  cells (Figure 2A;  $p < 0.001$ ). The somewhat higher capacity of parental wild-type cells compared to nontransformed fibroblasts to form colonies is consistent with the established ability of ES cells to form teratomas [6].

To determine whether KIF4 KO cells are able to give rise to tumors in a more physiological setting, we introduced KIF4 KO cells into nude mice (Figure 2B). Tumors appeared within six days and increased in size and number over the next 15 days (Figure 2B). The ability of KIF4 KO cells to form tumors was similar to that of HA-Ras-transformed NIH-3T3 cells (data not shown). In control mice injected with parental ES cells, only a few, significantly smaller tumors were detected during the same period ( $p < 0.001$ ; Figure 2B). Compared to tumor tissue derived from control cells, tumor tissue derived from mice injected with KIF4 KO cells showed a significantly increased proportion of proliferating cells ( $p = 0.0018$ ; Figures 2C and 2D), but no significant difference in apoptotic cells was detected (data not shown), suggesting that tumor formation was due to hyperproliferation of KIF4 KO cells. We conclude that loss of KIF4 increases the potential of ES cells for tumor formation.

To determine whether loss of KIF4 was relevant to human tumors, we probed the NCI-60 tumor cell line collection for human KIF4 by Western blotting (Fig-2E). KIF4 was entirely absent or expressed at low levels in 35% (14/40) of tested tumor samples. No or reduced levels of KIF4 was found in tumors from the ovary (4/6), lung (1/6), breast (1/6), and CNS (1/2), and in renal tumors (3/4), melanoma (3/4), and leukemia (3/6). No reduction of KIF4 was found in colon cancer cell lines (0/7) (Figure 2E). The variations in KIF4 levels among tumor samples were specific because comparable levels of the protein were detected in tissues from healthy individuals and in several randomly selected cell lines and human tissue extracts (Figure S2).

### **KIF4 Disruption in Mouse ES Cells Activates Spindle Checkpoints and Causes Centrosome Supernumerary**

Next, we sought to explore the mechanism by which loss of KIF4 gives rise to tumors. Because KIF4 KO cells were still able to proliferate despite the presence of significant chromosomal defects and aneuploidy, we hypothesized that cell-cycle checkpoints were overridden in KIF4 KO cells. Indeed, KIF4 KO cells showed activation of spindle-assembly checkpoints (Figures 3A and 3B). The checkpoint sensor protein Mad2 was, in addition to its localization to centrosomes, associated with misaligned chromosomes in KIF4 KO cells and partially colocalized in these cells with the kinetochore marker CREST (Figure 3A, inset). In contrast, Mad2 in control cells was typically found only at the spindle poles and was absent from kinetochores (Figure 3B). Similarly, the spindle-checkpoint protein BubR1 was associated with hypercondensed chromosomes in KIF4 KO cells but was absent from kinetochores in control cells (Figure 3B, inset). Because KIF4 in normal cells is present all along the length of the chromosome arms, it is possible that loss of KIF4 and the observed hypercondensation of mitotic chromosomes affects spindle-microtubule attachment sites, tensions, or both, and thus leads to activation of the mitotic spindle checkpoints in KIF4 KO cells [7].

Centrosome amplification and structural abnormalities of centrosomes are commonly found in tumor cells [8,9]. Although it is not clear whether centrosomal defects are a cause or consequence of cancerous transformation, formation of supernumerary centrosomes can lead to mitotic abnormalities and multipolar spindles [10,11]. Because multipolar spindles are often found in KIF4 KO cells, we determined the status of centrosomes in these cells. We found that  $34\% \pm 3\%$  of KIF4 KO cells have numerical aberrations of centrosomes compared to  $0.5\% \pm 0.05\%$  of control parental cells (Figures 3C and 3D). KIF4 KO cells often contained between three and six centrosomes as opposed to the two normally found in mitotic control ES cells ( $p$

< 0.0001; Figures 3C and 3D). Centrosome supernumerary may arise from centrosome fragmentation or polyploidization, although the rate of aneuploidy was significantly higher (70%) than the percentage of cells containing supernumerary centrosomes (34%). In addition, centrosomes in KIF4 KO cells were often structurally abnormal, showing irregular shapes and coalescence of multiple centrosomes (Figures 3C and 3D). Therefore, consistent with the observed aneuploidy and their ability to form tumors, KIF4-depleted cells exhibit centrosome abnormalities.

### Activation of DNA-Damage Checkpoints upon Loss of KIF4

A recently discovered fundamental hallmark of cells with tumor potential and early tumor cells is the activation of DNA-damage response pathways [12,13]. It has been suggested that activation of these pathways serves as a surveillance mechanism to eliminate cells with tumorigenic potential and that defects in these pathways allow escape of tumorigenic cells [12,13]. Thus, we asked whether loss of KIF4 results in activation of DNA-damage response pathways (Figure 4). Consistent with their activation, phosphorylated histone  $\gamma$ H2AX and activated ATM kinase, two early DNA damage sensors, accumulated extensively in mitotic chromosomes in KIF4 KO cells (Figures 4A and 4B). In contrast, significantly lower but detectable levels of  $\gamma$ H2AX and no activated ATM kinase were found on chromosomes of control cells (Figures 4A and 4B). We demonstrated the general activation of DNA-damage response pathways by Western blotting of whole-cell extracts. KIF4 KO cells showed high levels of phosphorylated  $\gamma$ H2AX and the early DNA-damage repair component NBS1 (Figures 4A and 4C). Both major DNA-damage response pathways acting via the ATM and the ATR kinases were activated in KIF4 KO cells as indicated by increased phosphorylation of ATM at S1981 and its downstream kinase Chk1 at S345 and by phosphorylation of Chk2 at T68 and its downstream target p53 on S15 in KIF4 KO cells (Figures 4B and 4C). Consistent with the view that activation of DNA damage pathways is a hallmark of early, but not late, tumor cells was the fact that no significant activation of most markers, with the exception of Chk1 and Chk2, was observed in tumors derived from the nude mice (Figure 4C).

To exclude the possibility that activation of DNA-damage response pathways in KIF4 KO cells was a secondary effect, we examined the status of the two DNA-damage response pathways in parental ES cells from which KIF4 had been depleted by RNAi for 24 hr (Figures 4A-4C). This time period is sufficient to reduce the cellular level of KIF4 by more than 80% but eliminates the possibility of artifactual long-term effects ([3]; data not shown). As we observed in KIF4 KO cells,  $\gamma$ -H2AX and phosphorylated ATM accumulated rapidly on mitotic chromosomes of KIF4-depleted cells but were absent in cells treated with control RNAi (Figures 4A and 4B). Western blotting confirmed the immediate activation of DNA-damage response pathways upon loss of KIF4 (Figure 4C).  $\gamma$ H2AX, NBS1, ATM, Chk1, Chk2, and p53 were all activated as indicated by their increased phosphorylation in RNAi-treated cells compared to control cells (Figure 4C). We conclude that activation of DNA-damage response pathways is an immediate response of cells to loss of KIF4.

### Discussion

We demonstrated here that loss of a molecular motor protein can lead to tumor formation. A physiological role for KIF4 in tumor formation is strongly suggested by its absence in 35% of randomly selected tumor cell lines. Furthermore, KIF4 has been found to be misexpressed in premalignant trophoblasts [14], and HKIF4A has recently been identified by microarray analysis as one of the most dramatically down-regulated genes in tumors with metastatic potential [15]. The observed activation of DNA-damage response pathways upon loss of KIF4 in cells is consistent with the recent realization that activation of these pathways is an early hallmark of cells with tumor potential [12,13]. These results extend earlier observations in cell culture showing that loss of other mitotic motors can lead to aneuploidy [16,17]. Our

observation of tumor formation via loss of a molecular motor is a novel concept in the fields of molecular motors and tumor biology.

Because the primary effects of loss of KIF4 are mitosis defects leading to aneuploidy, our results support the notion that aneuploidy can trigger tumorigenesis [18,19]. Although the mechanisms by which aneuploidy causes tumors is unclear, likely candidates are stochastic reduction of tumor-suppressor gene dosage and oncogene amplification due to changes in copy number. Although our observations suggest that aneuploidy can act as the first step in tumor formation, they do not show that it is in itself sufficient for the formation of tumors. In particular, the observed centrosome amplifications might be a consequence of KIF4 deletion and might be instrumental in the early process of tumor formation [9,20]. Similarly, we also can not rule out the presence of other secondary events, such as mutations in tumor suppressors, upon loss of KIF4. However, these would be downstream events facilitated by the aneuploid nature of KIF4 KO cells. Finally, it remains to be determined how faithfully the hyperproliferative tumors in nude mice represent human tumors.

The mechanism for KIF4-loss-mediated tumorigenesis is likely to be directly linked to its role in mitosis. Loss of KIF4 leads to numerous mitotic defects, including chromosome hypercondensation, aberrant spindle formation, anaphase bridges, defective cytokinesis, and aneuploidy [3-5]. Any of these defects may activate mitotic checkpoints and DNA-damage response pathways. Although many cells with defective mitoses will be eliminated by apoptosis or subsequent cell-cycle arrest, some KIF4 KO cells with genomic defects may escape these checkpoints, allowing them to proliferate and to form tumors [12,21]. This scenario is consistent with previous observations indicating that loss of human KIF4A does not lead to a complete block in cell-cycle progression but merely to a slowed progression through mitosis [3]. One might then predict that any defects that lead to slippage of cells with genomic defects through mitosis can give rise to tumor cells. [22,23]. Indeed, heterozygotic loss of Mad2 or BubR1, which weakens but does not completely eliminate mitotic checkpoints, results in aneuploidy, and in some cases increases tumor formation [24-30]. These considerations strongly support the emerging view that slippage of aneuploid cells through mitosis is a potent mechanism of tumor formation [22].

#### Acknowledgments

We thank T. Yen, T. Kapoor, and A. Nussenweig for providing antibodies, D. Lowy for providing NIH 3T3 and HA-Ras-transformed cells, and Tatiana Karpova for helping with microscopy. Imaging was performed at the National Cancer Institute Fluorescence Imaging Facility. This research was supported by the Intramural Research Program of the National Institutes of Health, National Cancer Institute, Center for Cancer Research.

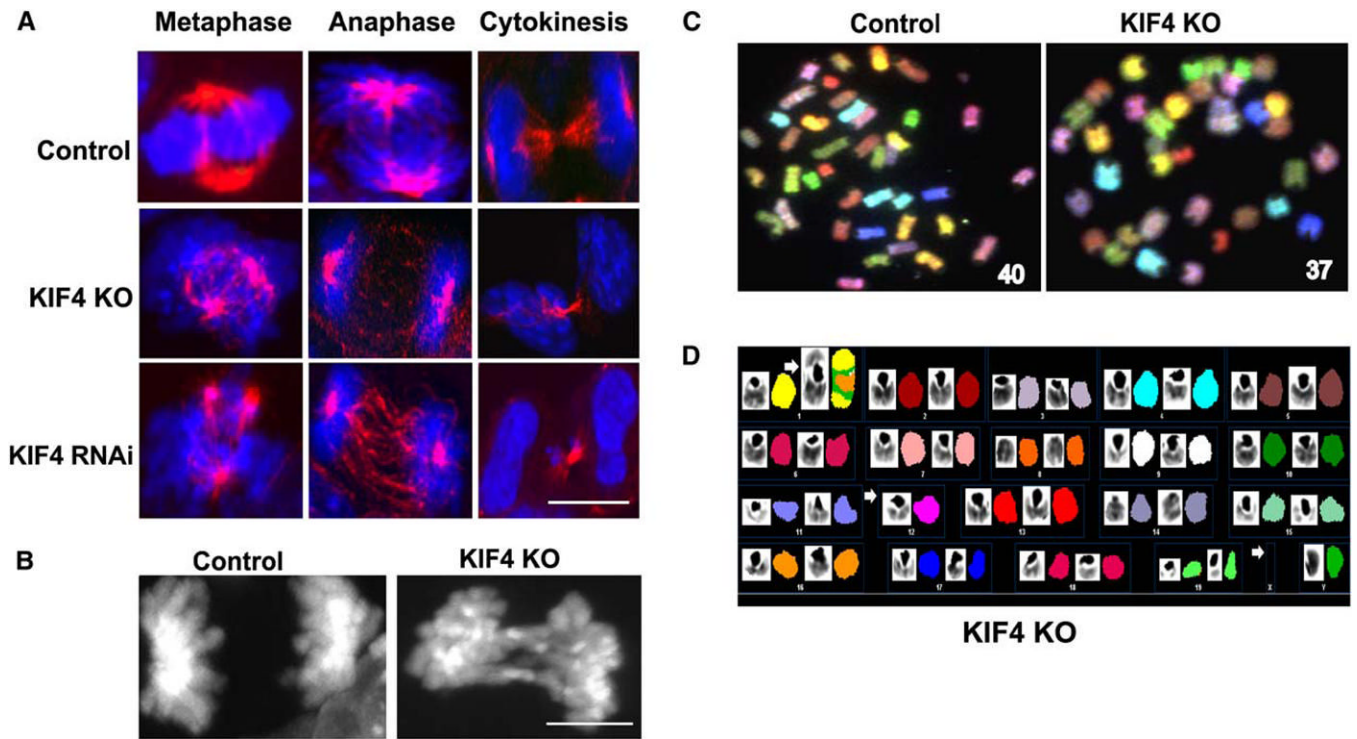
#### References

1. Lawrence CJ, Dawe RK, Christie KR, Cleveland DW, Dawson SC, Endow SA, Goldstein LS, Goodson HV, Hirokawa N, Howard J, et al. A standardized kinesin nomenclature. *J. Cell Biol* 2004;167:19–22. [PubMed: 15479732]
2. Mazumdar M, Misteli T. Chromokinesins: Multital-ented players in mitosis. *Trends Cell Biol* 2005;15:349–355. [PubMed: 15946846]
3. Mazumdar M, Sundareshan S, Misteli T. Human chromokinesin KIF4A functions in chromosome condensation and segregation. *J. Cell Biol* 2004;166:613–620. [PubMed: 15326200]
4. Kurasawa Y, Earnshaw WC, Mochizuki Y, Dohmae N, Todokoro K. Essential roles of KIF4 and its binding partner PRC1 in organized central spindle midzone formation. *EMBO J* 2004;23:3237–3248. [PubMed: 15297875]
5. Castoldi M, Vernos I. Chromokinesin Xklp1 contributes to the regulation of microtubule density and organization during spindle assembly. *Mol. Biol. Cell* 2006;17:1451–1460. [PubMed: 16407411]
6. Smith AG. Embryo-derived stem cells: Of mice and men. *Annu. Rev. Cell Dev. Biol* 2001;17:435–462. [PubMed: 11687496]

7. Pinsky BA, Biggins S. The spindle checkpoint: Tension versus attachment. *Trends Cell Biol* 2005;15:486–493. [PubMed: 16084093]
8. D'Assoro AB, Lingle WL, Salisbury JL. Centrosome amplification and the development of cancer. *Oncogene* 2002;21:6146–6153. [PubMed: 12214243]
9. McDermott KM, Zhang J, Holst CR, Kozakiewicz BK, Singla V, Tlsty TD. p16(INK4a) prevents centrosome dysfunction and genomic instability in primary cells. *PLoS Biol* 2006;4:e51.
10. Brinkley BR. Managing the centrosome numbers game: From chaos to stability in cancer cell division. *Trends Cell Biol* 2001;11:18–21. [PubMed: 11146294]
11. Sluder G, Nordberg JJ. The good, the bad and the ugly: The practical consequences of centrosome amplification. *Curr. Opin. Cell Biol* 2004;16:49–54. [PubMed: 15037304]
12. Bartkova J, Horejsi Z, Koed K, Kramer A, Tort F, Zieger K, Guldberg P, Sehested M, Nesland JM, Lukas C, et al. DNA damage response as a candidate anti-cancer barrier in early human tumorigenesis. *Nature* 2005;434:864–870. [PubMed: 15829956]
13. Gorgoulis VG, Vassiliou LV, Karakaidos P, Zacharatos P, Kotsinas A, Liloglou T, Venere M, Dittullo RA Jr. Kastrinakis NG, Levy B, et al. Activation of the DNA damage checkpoint and genomic instability in human precancerous lesions. *Nature* 2005;434:907–913. [PubMed: 15829965]
14. Lee BP, Rushlow WJ, Chakraborty C, Lala PK. Differential gene expression in premalignant human trophoblast: Role of IGFBP-5. *Int. J. Cancer* 2001;94:674–684. [PubMed: 11745462]
15. Montel V, Huang TY, Mose E, Pestonjamas K, Tarin D. Expression profiling of primary tumors and matched lymphatic and lung metastases in a xenogeneic breast cancer model. *Am. J. Pathol* 2005;166:1565–1579. [PubMed: 15855655]
16. Weaver BA, Bonday ZQ, Putkey FR, Kops GJ, Silk AD, Cleveland DW. Centromere-associated protein-E is essential for the mammalian mitotic checkpoint to prevent aneuploidy due to single chromosome loss. *J. Cell Biol* 2003;162:551–563. [PubMed: 12925705]
17. Mailhes JB, Mastromatteo C, Fuseler JW. Transient exposure to the Eg5 kinesin inhibitor monastrol leads to syntelic orientation of chromosomes and aneuploidy in mouse oocytes. *Mutat. Res* 2004;559:153–167. [PubMed: 15066583]
18. Jefford CE, Irminger-Finger I. Mechanisms of chromosome instability in cancers. *Crit. Rev. Oncol. Hematol* 2006;59:1–14. [PubMed: 16600619]
19. Kops GJ, Weaver BA, Cleveland DW. On the road to cancer: aneuploidy and the mitotic checkpoint. *Nat. Rev. Cancer* 2005;5:773–785. [PubMed: 16195750]
20. Pihan GA, Wallace J, Zhou Y, Doxsey SJ. Centrosome abnormalities and chromosome instability occur together in pre-invasive carcinomas. *Cancer Res* 2003;63:1398–1404. [PubMed: 12649205]
21. Duensing S, Munger K. Centrosome abnormalities and genomic instability induced by human papillomavirus onco-proteins. *Prog. Cell Cycle Res* 2003;5:383–391. [PubMed: 14593733]
22. Weaver BA, Cleveland DW. Decoding the links between mitosis, cancer, and chemotherapy: The mitotic checkpoint, adaptation, and cell death. *Cancer Cell* 2005;8:7–12. [PubMed: 16023594]
23. Tao W, South VJ, Zhang Y, Davide JP, Farrell L, Kohl NE, Sepp-Lorenzino L, Lobell RB. Induction of apoptosis by an inhibitor of the mitotic kinesin KSP requires both activation of the spindle assembly checkpoint and mitotic slippage. *Cancer Cell* 2005;8:49–59. [PubMed: 16023598]
24. Cheung HW, Jin DY, Ling MT, Wong YC, Wang Q, Tsao SW, Wang X. Mitotic arrest deficient 2 expression induces chemosensitization to a DNA-damaging agent, cisplatin, in nasopharyngeal carcinoma cells. *Cancer Res* 2005;65:1450–1458. [PubMed: 15735033]
25. Kops GJ, Foltz DR, Cleveland DW. Lethality to human cancer cells through massive chromosome loss by inhibition of the mitotic checkpoint. *Proc. Natl. Acad. Sci. USA* 2004;101:8699–8704. [PubMed: 15159543]
26. Michel LS, Liberal V, Chatterjee A, Kirchweger R, Pasche B, Gerald W, Dobles M, Sorger PK, Murty VV, Benzra R. MAD2 haplo-insufficiency causes premature anaphase and chromosome instability in mammalian cells. *Nature* 2001;409:355–359. [PubMed: 11201745]
27. Michel L, Benzra R, Diaz-Rodriguez E. MAD2 dependent mitotic checkpoint defects in tumorigenesis and tumor cell death: A double edged sword. *Cell Cycle* 2004;3:990–992. [PubMed: 15254432]

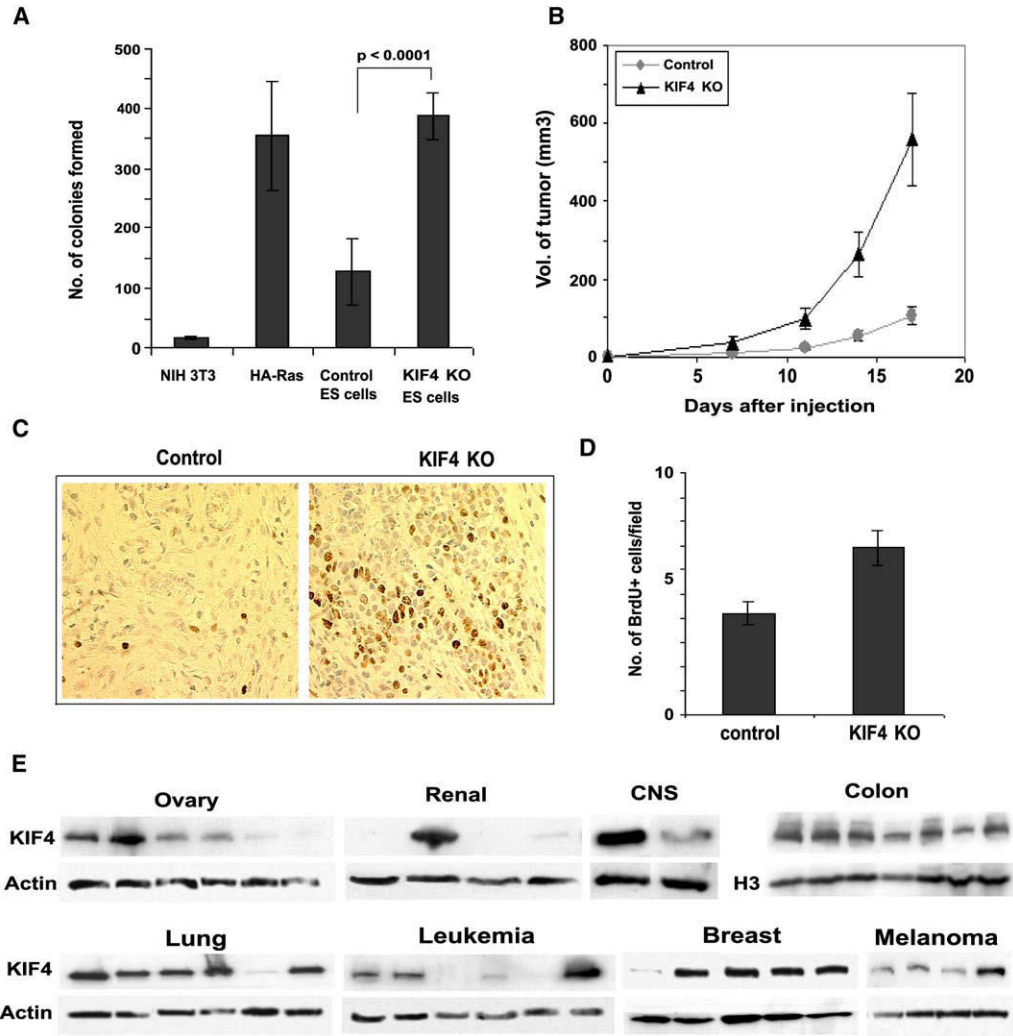
28. Hanks S, Coleman K, Reid S, Plaja A, Firth H, Fitzpatrick D, Kidd A, Mehes K, Nash R, Robin N, et al. Constitutional aneuploidy and cancer predisposition caused by biallelic mutations in BUB1B. *Nat. Genet* 2004;36:1159–1161. [PubMed: 15475955]
29. Musio A, Montagna C, Zambroni D, Indino E, Barbieri O, Citti L, Villa A, Ried T, Vezzi P. Inhibition of BUB1 results in genomic instability and anchorage-independent growth of normal human fibroblasts. *Cancer Res* 2003;63:2855–2863. [PubMed: 12782591]
30. Baker DJ, Jegannathan KB, Cameron JD, Thompson M, Juneja S, Kopecka A, Kumar R, Jenkins RB, de Groen PC, Roche P, et al. BubR1 insufficiency causes early onset of aging-associated phenotypes and infertility in mice. *Nat. Genet* 2004;36:744–749. [PubMed: 15208629]





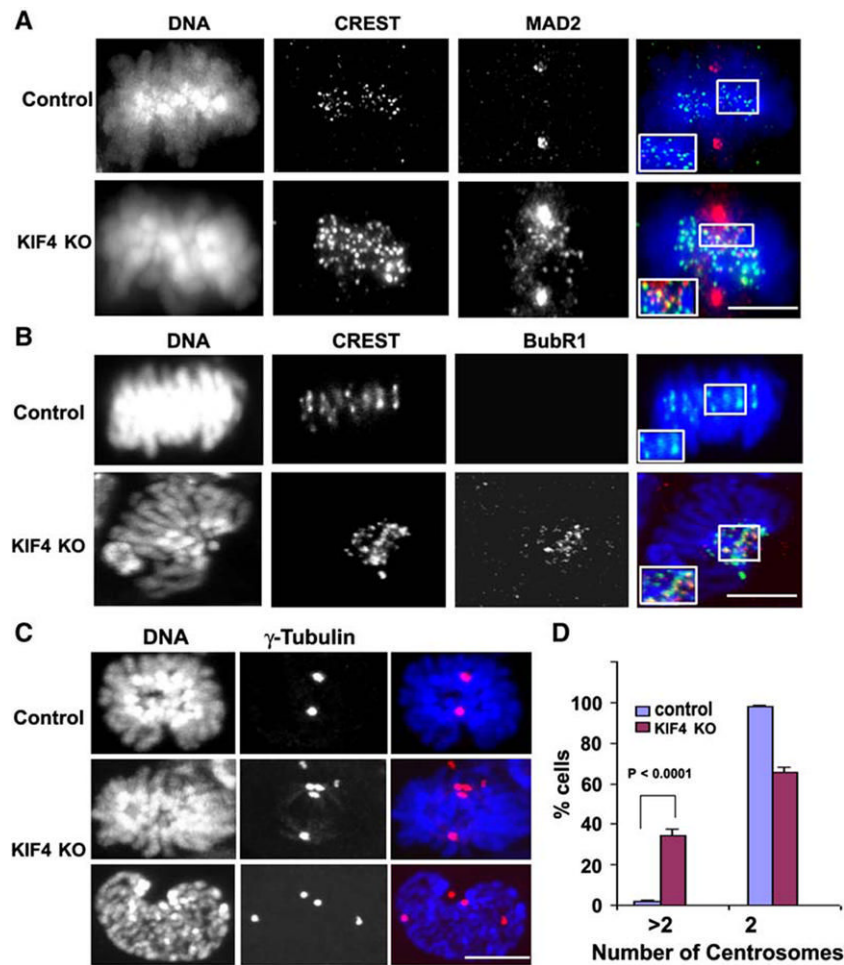
**Figure 1.**

KIF4 Knockout Mouse ES Cells Have Mitotic Defects and Aberrant Chromosome Structure and Are Aneuploid (A) Mitotic defects in all phases of mitosis. Microtubules (red); DNA (blue). The scale bar represents 5  $\mu$ m. (B) Anaphase bridge formation in KIF4 KO cells. DAPI (white). The scale bar represents 5  $\mu$ m. (C) Chromosome hypercondensation and aneuploidy in KIF4 KO cells. Metaphase spreads of parental control and KIF4 KO cells reveal hypercondensation and frequent aneuploidy upon loss of KIF4. The number of chromosomes in the spread is indicated. (D) Spectral karyotyping of KIF4 KO cells. A representative karyotype from a SKY analysis of KIF4 KO ES cells displaying the pseudocolored image and the corresponding inverted DAPI image for each chromosome. The numbers at the bottom of each box represent the chromosome number. A KIF4 KO cell with a pseudodiploid karyotype lacking chromosome X and one homolog of chromosome 12 (white arrows). The arrow in box 1 indicates a complex Robertsonian translocation involving chromosomes 1 and 16, respectively, to give a complex karyotype of 38, -X, Y, Rb[1; T(16;1)],-12.

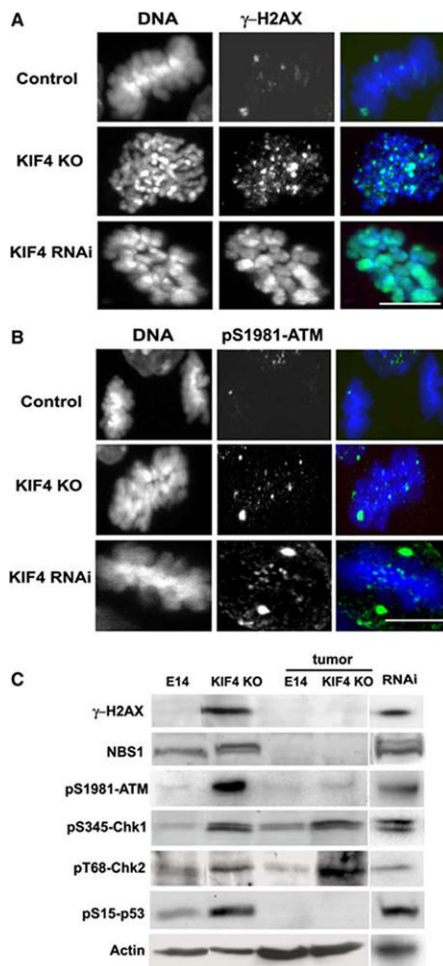


**Figure 2.** KIF4 KO ES Cells Have the Potential to Form Tumors (A) Soft-agar colony-formation assay with NIH 3T3 cells (negative control), HA-Ras-transformed cells (positive control), parental ES cells (negative control), and the KIF4 KO ES cells in triplicates. Anchorage-independent growth was measured by quantification of the number of colonies formed per  $10^4$  cells plated. Values represent averages  $\pm$ SD from three experiments with triplicate plates. (B) Tumor formation by control ES and KIF4 KO ES cells in nude mice. Control ES and KIF4 KO ES cells ( $5 \times 10^6$  cells per site) were injected subcutaneously into two flank sites of each nude mouse (five mice per group). Mice were examined for tumor formation, and tumor size was measured at the indicated time. Tumor volume is presented as the mean volume ( $\text{mm}^3$ )  $\pm$ SD of tumors from ten injection sites per group. (C) Proliferation of tumor cells. Anti-BrdU immunostaining of tumors of the indicated genotypes in nude mice. Magnification is  $\times 400$ . (D) Proliferation rates in control ES and KIF4 KO ES tumors. We quantified tumor cell proliferation by counting BrdU-labeled cells on histological sections. Results are the mean  $\pm$ SEM for a minimum of five tumors of each genotype. (E) KIF4 protein-expression profiling in human cancer cell lines. The NCI-60 set of cancer cell lines was tested with Western blots for KIF4 protein. Fourteen of forty cell lines showed lower KIF4 expression or complete loss of KIF4 expression. Actin or core histone H3 was used as loading controls.





**Figure 3.** Centrosome Aberrations and Activation of Spindle Checkpoints in KIF4 KO Cells (A) Activation of mitotic checkpoints in KIF4 KO cells. MAD2 (red) in control cells, localizes at centrosomes but is absent from kinetochores identified by anti-CREST antibody (green). In KIF4 KO cells, CREST and MAD2 partially colocalize (inset). Scale bars represent 5 $\mu$ m. (B) BubR1 is found on kinetochores of KIF4 KO cells but not in control cells (inset). Scale bars represent 5 $\mu$ m. (C) Confocal-microscopy analysis of fixed parental E14 and KIF4 KO cells at various stages of mitosis. Multiple centrosomes or coalescence of two or more centrosomes are frequently observed in KIF4 KO ES cells. Centrosomal marker protein  $\gamma$ -tubulin is in red, and DNA is in blue. Scale bars represent 5 $\mu$ m. (D) Quantitation of centrosomal numerical abnormalities. A minimum of 100 cells were counted from ten randomly chosen fields from each of three different samples. The values represent averages  $\pm$ SD.

**Figure 4.**

DNA-Damage Pathways Are Activated in KIF4 KO ES Cells (A and B) Confocal immunofluorescence microscopy images of control, KIF4 KO ES, and parental ES cells depleted of KIF4 by RNAi for 24 hr. Cells are stained for  $\gamma$ -H2AX or pS1981-ATM (green) and DNA (blue). KIF4 KO and KIF4 RNAi ES cells showed both  $\gamma$ -H2AX and pS-ATM foci, indicating activation of the DNA-damage pathway in these cells. Scale bars represent 5 $\mu$ m. (C) Immunoblot analysis of total cell extracts from control cells, KIF4 KO ES cells, tumors derived from nude mice injected with control and KIF4 KO ES cells, and parental ES cells depleted of KIF4 for 24 hr. Actin was used as the loading control.